CHAPTER 296

Numerical Modeling of Nearshore Morphological Changes under a Current-Wave Field

Taerim Kim[1] and Hsiang Wang[2]

Abstract

This paper presents a time-dependent 3-D nearshore morphological response numerical model which includes the slope effect, undertow current, wave-borne transport, and transition zone effect. These effects are very important but often not estimated in other sediment transport models. By including the cushioning effect in the water column, which prevents the advection of turbulence generated by wave breaking from the surface to the bottom, this model is shown to be able to approach an equilibrium state of sediment transport. The computed cross-shore and longshore sediment transport rates are calibrated based on the large wave tank data, 3-D basin experiments, and available sediment transport formulas. The predicted changes of bottom topography near structures and inlet in physical model are compared for model verification.

Introduction

Prediction of beach response to the engineering activities is important for assessing the impact of coastal structures and to improve their design. It is also useful for evaluating remedial and mitigation measures. Numerical modeling is clearly an attractive alternative for this purpose and is becoming increasingly viable with the advancement of computational facilities and improved understanding on wave mechanics and sediment transport processes.

There have been two types of approach to predict the 3- dimensional morphological changes in the nearshore zone. The so called 3DBEACH (3-dimensional decoupled model of beach change) by Larson et al. (1989) utilizes the profile change model, SBEACH, for calculating storm-induced beach erosion and recovery and the shoreline change model, GENESIS, for calculating long-term change in shoreline position. Since the profile model is based on equilibrium profile, the combined model also maintains

1 Senior Research Engineer, Ocean Engineering Division, KORDI, Ansan, P.O. Box 29, SEOUL 425-600, KOREA
2 Professor, Department of Coastal and Oceanographic Engineering, University of Florida, Gainesville, FL 32611, USA

the ability to approach an equilibrium bottom configuration under steady wave condition. This is difficult to attain in the models of other type. However, since the submodels are all wave driven, combined current wave effect can not be directly addressed. The other approach computes nearshore topographic change based on local sediment flux balance. This approach usually links a hydrodynamic submodel with a sediment transport submodel. Models of this kind with varying degrees of sophistication have been developed. van Rijn et al. (1989) estimated the sediment transport rate by multiplying the wave-averaged mean vertical sediment concentration by the wave-averaged local horizontal velocity. In their model, the wave-borne transport mechanism is not directly addressed. A model developed by Ohnaka and Watanabe (1990), on the other hand, computes the flow field with considerations of current and wave interaction based on coupled mild-slope wave equation and depth-averaged circulation equations. It calculates the rate of sediment transport as the summation of two energetic mechanisms, one due to the mean current and the other due to waves (Watanabe et al., 1986). Recently, the nearshore circulation model was improved by a 3-D approach, which employed a combined depth-integrated current model and a vertical profile model(De Vriend and Stive, 1987). This improvement when incorporated into the sediment transport model enables one to more realistically represent the 3-D nature both inside and outside the surfzone. Briand and Kamphius (1993) multiplied the time averaged quasi-3D velocities to a time averaged exponential sediment concentration profile to achieve a 3-D sediment flux. This technique of combining a quasi-3D velocity profile with a vertical distribution of suspended sediment concentrations is a promising step to lead to full 3-D models in the future.

The model developed in this study consists of three submodels for calculation of waves, nearshore currents, and beach changes. At the first step, the initial beach topography and the geometry of the structures for the study area are given as input data. Next, the wave model determines the spatial
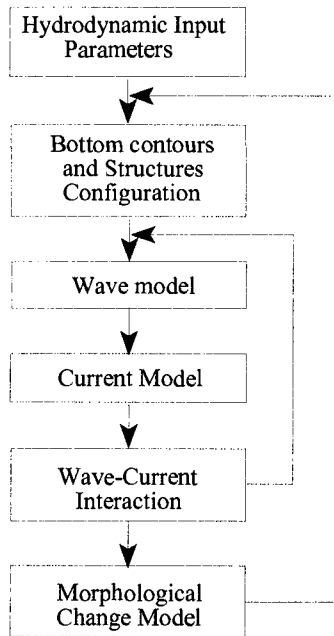
Figure 1 Structure of Nearshore Morphodynamic Model.

distributions of radiation stresses and near-bottom orbital velocities for a given incident wave condition. Then, the circulation model computes the mean water surface level and the depth-averaged mean currents using depth-averaged momentum and continuity equations. Inside the surf zone, mean undertow current, transition zone length, and cushioning effect are calculated based on the wave-current model results. Spatial distribution of sediment transport fluxes are computed in the domain of interest. Finally, bottom topography changes are computed based on sediment mass conservation. The change in bottom topography will modify the flow field. Therefore the hydrodynamic model needs to be updated from time to time. Figure 1 shows the computational flow chart of the model.

Wave and Circulation Models

The flow field in the nearshore is computed by depth integrated 2-D hydrodynamic model developed by Winer(1988). The hydrodynamic model consists of wave and circulation models which are fully coupled through interaction terms. First, the wave model determines the spatial distributions of radiation stresses and near-bottom orbital velocities based on the following parabolic wave equation,

$$(C_g\cos\theta + U)A_x + \frac{\sigma}{2}\left(\frac{C_g\cos\theta + U}{\sigma}\right)_x A + VA_y + \frac{\sigma}{2}\left(\frac{V}{\sigma}\right)_y A$$
$$-\frac{i}{2}kC_g(1-\cos^2\theta)A - \frac{i}{2}\left[CC_g\left(\frac{A}{\sigma}\right)_y\right]_y + \frac{W}{2}A = 0 \tag{1}$$

where, U and V are the depth averaged horizontal velocities in the x (cross-shore) direction and y (longshore) direction, respectively, C is the phase velocity, C_g is the group velocity, σ is the intrinsic angular frequency, A is the complex amplitude , θ is the angle of the wave propagation relative to the x axis, the subscripts x and y denote derivatives in the x and y directions, respectively, W is the energy dissipation coefficient. The coefficient W is related to the energy dissipation due to wave breaking following the work of Dally et al., (1984).

$$D_E = \frac{K}{D}[(E-E_s)C_g] \tag{2}$$

where, D_E is the energy dissipation rate, D is water depth, K is empirical parameter (K=0.17) , E is the local wave energy density, E_s is the local stable wave energy density that the breaker is striving to attain.

The circulation model computes the mean water surface level and the depth averaged mean currents using depth averaged momentum and continuity equations with the radiation stresses imported from the wave model as the driving force.

The governing equations are given by (Ebersole and Dalrymple, 1979)

$$\frac{\partial U}{\partial t} + U\frac{\partial U}{\partial x} + V\frac{\partial U}{\partial y} + g\frac{\partial \bar{\eta}}{\partial x} + \frac{1}{\rho D}\tau_{bx} - \frac{1}{\rho D}\tau_{sx}$$

$$+ \frac{1}{\rho D}\left(\frac{\partial S_{xx}}{\partial x} + V\frac{\partial S_{xy}}{\partial y}\right) + \frac{1}{\rho}\frac{\partial \tau_l}{\partial y} = 0$$

$$\frac{\partial V}{\partial t} + U\frac{\partial V}{\partial x} + V\frac{\partial V}{\partial y} + g\frac{\partial \bar{\eta}}{\partial y} + \frac{1}{\rho D}\tau_{by} - \frac{1}{\rho D}\tau_{sy}$$

$$+ \frac{1}{\rho D}\left(\frac{\partial S_{xy}}{\partial x} + V\frac{\partial S_{yy}}{\partial y}\right) + \frac{1}{\rho}\frac{\partial \tau_l}{\partial x} = 0$$

(3)

and the continuity equation

$$\frac{\partial \bar{\eta}}{\partial t} + \frac{\partial}{\partial x}(UD) + \frac{\partial}{\partial y}(VD) = 0 \tag{4}$$

where, t is the time; x and y are the Cartesian coordinates in a horizontal plane; U and V are the corresponding velocity components of the nearshore current; $D = h + \bar{\eta}$; h is the still water depth; $\bar{\eta}$ is the elevation of the mean water level due to wave set up/set down; τ_l is the lateral shear stress due to turbulent mixing; τ_{bx} and τ_{by} are the bottom shear stresses; τ_{sx} and τ_{sy} are the surface shear stresses; and S_{xx}, S_{xy}, and S_{yy} are the radiation stress components which arise from the excess momentum flux due to waves. These equations are obtained by integrating the local x and y momentum equations and the continuity equation over the depth of the water column and then time-averaging the results. The governing equations in the circulation model are solved by a matrix analysis using the alternating direction implicit (ADI) scheme (Winer, 1988). In order to treat the wave-current interaction, waves and currents are calculated alternatively.

Inside the surf zone, the 2-D model is inadequate as the model will yield null current in the cross-shore direction, consequently, zero net cross-shore transport. In reality, the current inside the surfzone is highly three dimensional. Field and laboratory observations of surf zone flow show the existence of current that is directed offshore on the bottom, balanced with the onshore flow of water carried by the breaking waves. This offshore-directed steady current near the bed, commonly referred to as undertow, is known to be the most important mechanism causing profile erosion and bar. The depth-integrated discharge of x component by undertow current, Q_u is expressed as

$$Q_u = \frac{\rho g H^2 k_x}{8\sigma} \tag{5}$$

The mean undertow velocity is simply estimated as $\bar{u} = Q_u/(\eta_c + h)$, which is directed offshore.

Sediment Transport Model

The computed current-wave field is used to drive the sediment model which, in turn, computes the morphological changes by utilizing the equation of conservation of sediment material. In the present study, the sediment transport formula contains two parts, bed load and suspended load. The bed load transport is based on an energetic approach driven by mean current and bottom wave orbital velocity. Owing to the asymmetric wave bottom orbital velocity in a wave cycle, this bed load transport by wave orbital velocity has a net onshore component. The suspended load transport which dominates in surfzone is built upon an undertow current. Here, the suspended sediment concentration is related to breaking wave energy dissipation and the transport velocity is the mean undertow current. This component is always directed offshore. The total transport Q is the sum of bed and suspended loads as followings

$$Q = q_b + q_s$$
$$q_b = A_{bc}(\tau_m - \tau_{cr})U_c/\rho g + A_{bw}(\tau_m - \tau_{cr})U_w/\rho g \qquad (6)$$
$$q_s = A_s \tau_{turb} Q_u$$

, where ρ is the density of water, g is gravity coefficient, U_c is the integrated depth mean wave induced-current, U_w is the maximum orbital velocity at the bottom, Q_u is the discharge by the undertow, τ_m is the maximum bottom shear stress generated by wave and current, τ_{turb} is the turbulent shear stress generated by waves and mean current, τ_{cr} is the critical shear stress under waves and mean current, A_{bc}, A_{bw}, and A_s are calibrated coefficients.

Sediment transport is influenced by the bottom slope as downslope reduces resistance and upslope increases resistance. The down-slope gravitational transport is the most important mechanism to keep the bed from growing indefinitely and , to enable the coastal profile to reach a dynamic equilibrium state. A basic formulation to express the slope gravitational transport component proposed by Horikawa (1988) assumes the following functional form,

$$q_x = q_x^1 + \varepsilon_x |q_x^1| \frac{\partial h}{\partial x}$$
$$q_y = q_y^1 + \varepsilon_y |q_y^1| \frac{\partial h}{\partial y} \qquad (7)$$

and in which q_x and q_y are the transport components in x and y directions, respectively, q_x^1 and q_y^1 are their equivalents for horizontal bed, h is the water depth and ε are empirical coefficients

The zone between the incipient breaking and the plunging point is defined as

transition zone. The transition zone effect on the wave setup, undertow current, and sediment transport is a subject of increased research over recent years. It showed that the inclusion of the transition zone in profile modeling has an important effect on the predicted profiles, particularly for the bar features. Several approaches have been proposed to evaluate the distance and influence of the transition zone based on wave tank experiments(Galvin (1969)). The present model uses the following formula analyzed from the experimental data(O'Shea et al. (1991)).

$$l_t = 0.556 \ \tan\beta \ L_b\xi^{-1.465} \tag{8}$$

in which, $tan\beta$ and L_b are respectively the bed slope and wave length at breaking, and ξ is the surfzone parameter.

Cushioning Effect

Most of the laboratory results as well as field evidence seems to support the concept of beach equilibrium. The profile equilibrium can be reached either when the tangential thrust by fluid is not strong enough to overcome the sand resistance or when the local landward sediment transport is balanced by the local seaward sediment transport. In the latter case, although there could be active sediment movement, the profile remains stable. Including this feature into the model is a difficult subject. One popular approach is to predesignate an equilibrium profile shape. The sediment transport formulas should then be consistent to lead the profile evolution to this equilibrium profile. Kriebel's (1985) storm profile model was of this kind .This type of models can be classified as closed loop model. On the other hand, most sediment transport models do not have a targeted equilibrium profile therefore often fail to reach an equilibrium state. This type of models is known as open loop model. For the open loop model to reach equilibrium, mechanisms must be devised to locally balance the on/offshore transport. The present model is an open loop model. In the formulas presented earlier, inside the surf zone the offshore transport is much too strong to be balanced by the onshore transport component. The reason is that in the formulation, once wave breaks wave breaking-induced turbulence immediately produces a strong bottom stress and the resulting offshore transport is much larger than the onshore transport computed by the bed load transport equation. Clearly, the offshore transport equation needs to be modified. Dally and Dean (1984) pointed out that the expression developed for the sediment concentration profile apparently lacks the ``cushioning'' effect which the water column provides in reducing the amount of sediment entrainment as breaking wave form and trough evolve. This cushioning effect is especially important in the stabilization of the bar and trough formation. Almost no work has been done for this cushioning effect. The present model attempted to incorporate this cushioning effect into the model based on the ratio of the depth and wave height at the plunging point as follows,

$$C_{us} = \tanh(7\frac{H}{D})^{700} \tag{9}$$

where, C_{us} is the cushioning effect, H is the wave height, D is the water depth. Figure 2(a) plots this cushioning coefficient and its effect on sediment transport. As can be seen, when relative water depth increases, the cushioning equation limits the turbulence penetration to the bottom. When wave height is larger than water depth, there is no cushioning effect. However, as the water depth at the trough zone becomes larger, cushioning effect becomes stronger. Finally when water depth reaches 2.5 times the wave height breaking induced turbulence will not reach the bottom. This equation is, of course, purely empirical at this stage with no supporting data. Figure 2(b) shows the effect on sediment transport rate. With the inclusion of this effect, the open loop model presented in this study could reach profile equilibrium without a predetermined profile shape.
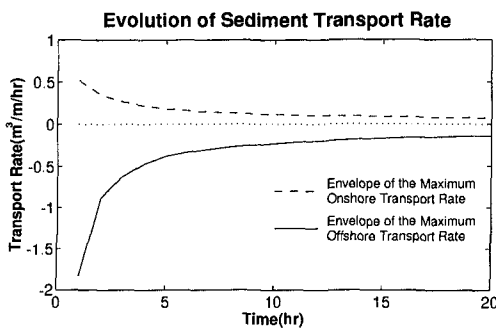
Calibration of Sediment Transport Rate

The nearshore sediment transport characteristics under storm wave conditions as predicted by the model are illustrated here. In order to validate the 3-D morphological response model, cross-shore transport rate and longshore transport rate are calibrated separately by using available experiment data or empirical formulas.

a)
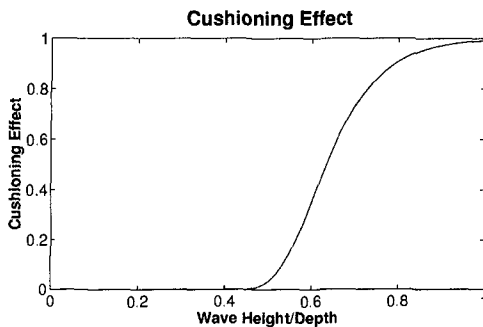
b)

Figure 2 a)Distribution of Cushioning Effect. b)Evolution of Sediment Transport Rate.
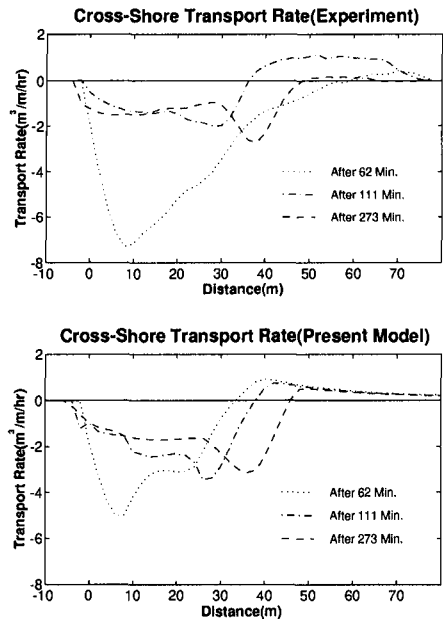
Cross-Shore Transport Rate

For the calibration of cross-shore transport rate, two sets of 2-D tank experiment data were used. These included the case of a sand beach backed by a sloping dike tested in the German Big Wave Flume (GWK) and case CE 400 from Saville's large wave tank tests (CE). Comparisons were made between computed values and experimental results both in profile changes and transport rates.

The GWK experiment(Dette and Uliczka, 1986) used sand with a median diameter of 0.33 mm and the test profile was subjected to regular wave attack (H=1.5 m, T=6 sec). Figure 3 shows the comparison between the predicted profiles and the experimental results at run times of 62, 111, and 273 minutes, respectively. The computed wave height distribution across shore

is also shown. The waves cut back the foreshore to produce a vertical scarp and a bar formed shoreward of the breaking point which grew and moved offshore with continued wave action. The numerical model satisfactorily reproduced the observed foreshore erosion and main breakpoint bar development. Simulated shoreline retreat and bar growth were initially rapid and gradually slowed as the bar moved offshore to reach a location close to that of the observed bar at the end of the run (20 hr). However, the bar trough is less well reproduced. All smaller features inshore of the main breakpoint bar were not reproduced in the simulations. Figure 4 shows the comparison of the cross-shore transport rate between the profile changes in Figure 3. Initially, a high peak appears near the shoreline as beach material slumps down slope into the foreshore zone in this experiment. These material was transported offshore to form the bar. The seaward changes of the peak transport rate explain the offshore movement of the bar. With the exception at the initial stage, the predicted transport rate distribution is in good agreement with the laboratory data. At the initial stage the experimental values were larger than predicted. There are many factors that could contribute to the difference such as slumping effect mentioned earlier. It was also found later in small scale experiments conducted at UF that the profile erosion particularly in the dune region was much more severe in the initial stage if the beach is dry and loosely compacted as opposed to wet and well compacted. The best overall fit of both profile
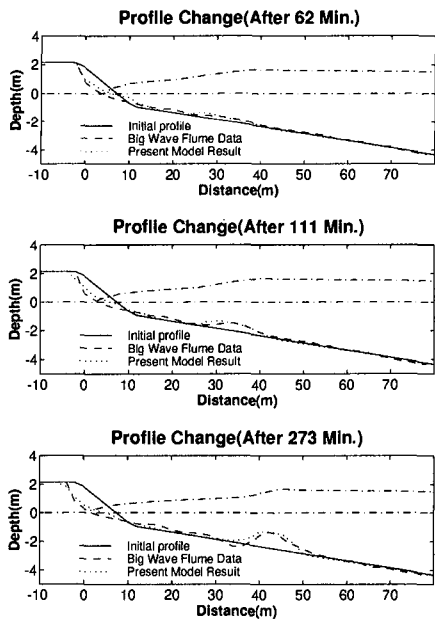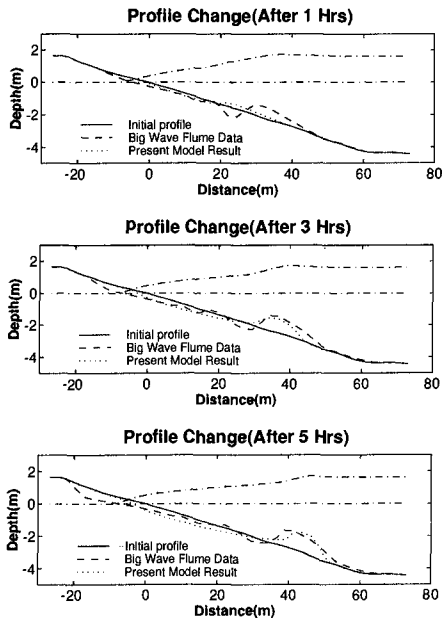

Figure 3 Comparison between Computed and Measured Beach Profiles for t= 62, 111, 273 minutes. Data from Dette and Uliczka (1986).
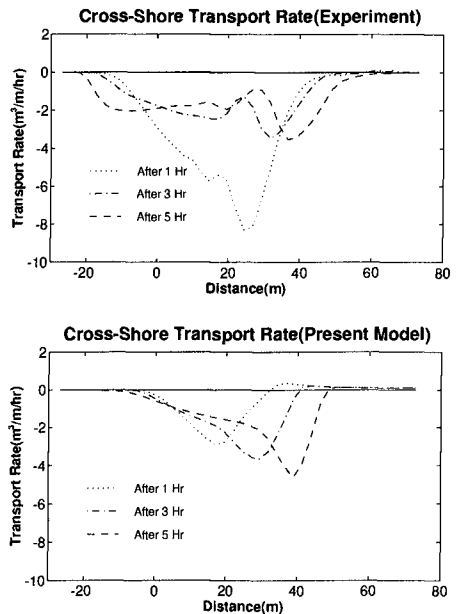
Figure 4 Comparison of Cross-Shore Transport Rates between Experiment and Present Model for t=62, 111, 273 minutes. Data from Dette and Uliczka(1986)

and transport rate was obtained by using A_{bw}

in a range from 0.05 to 0.07 and A_s from 1.0 x 10^{-5} (m^2/N) to 1.5 x 10^{-5} (m^2/N). With these determined A_{bw} and A_s values, the model was used to simulate the CE case CE400. Figure 5 shows the comparison of measured and calculated profiles. The test conditions were: initial uniform slope = 1/15; grain size = 0.22 mm; wave height and period of 1.62 m and 5.6 sec. The numerical and test results are shown for simulation times of 1, 3, and 5 hours. In this case, the bar development was also well predicted except at the initial stage. However, the profile change near the shoreline shows very different results between the experiment and the model. In experiment, there was strong erosion at the foreshore region above the water level, but this erosion was limited near the shoreline in the numerical model. The spatial distribution of the transport rate from the CE tests were very different from that of the GWK tests. Here in the CE case, peak transport initially occurred near the breaking point and did not show any onshore transport outside the breaking point (The numerical model results did show a very small onshore transport component). Also, in the CE experiments, the transport in swash zone apparently played an important role to cause shore face erosion. The numerical model does not have an appropriate swash zone transport mechanism. Therefore, it was unable to reproduce the large erosion near the shoreline in the experiment.

Figure 5 Comparison between Calculated and Measured Beach Profiles for t= 1, 3, 5 hours. Data from Saville(1957).

Figure 6 Comparison of Cross-Shore Transport Rates between Experiment and Present Model for t=1,3,5 hours. Data from Saville(1957)
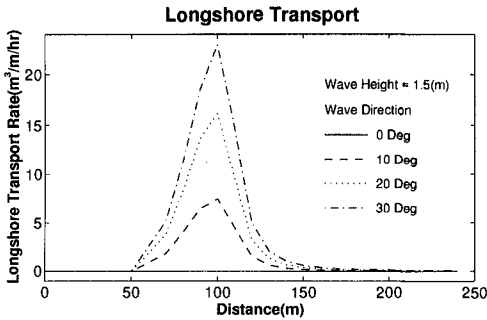
Longshore Transport Rate

Longshore sediment transport plays a very important role particularly in long term beach evolution. The longterm evolution of many coastlines is the result of slight gradients in the longshore transport rate. Available data suitable for calibration and verification of longshore transport rate are scarce and mostly limited to 2-D cases. The 2-D data will not yield information on A_{bc}. In this section, the characteristics of longshore transport rate are investigated by comparing with CERC formula and the coefficient A_{bc} was calibrated based on a 3-D basin experiment. The CERC's littoral drift formula (Shore Protection Manual, 1984) has the following form as,
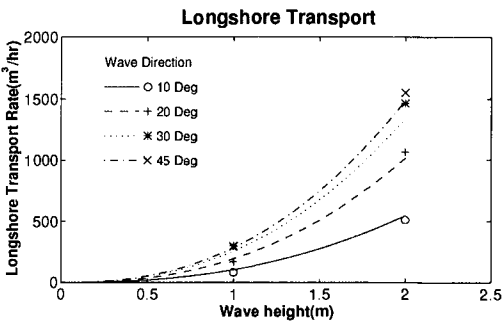
$$Q = \frac{K(EC_g\cos\theta\sin\theta)_b}{\rho g(s-1)(1-p)} \tag{10}$$

where Q is the volumetric longshore transport rate, E is wave energy, C_g is group velocity, s is specific gravity, p is porosity and K is an empirical transport coefficient. The formula is based on energetic concept with empirically determined coefficient based on field evidence.

In the present model, the sediment transport formulas as presented are of very different nature. However, for lack of laboratory and/or field data for verification, CERC's formula is used here as a bench mark to test the model. A case of 2-D beach that has an initial profile of a uniform slope (1/20) was used here to compare the characteristics of the present model and CERC's formula. Figure 7(a) shows the longshore transport distribution across the surf zone as calculated by the model at different wave angles under the same wave height of 1.5 m. The transport patterns are all bell-shaped with a uni-modal peak inside the breaking point. This shape is consistent with observations on beaches of more or less uniform slopes excluding the swash zone (dual peaks were common if swash zone is included). It is also shown that the longshore transport rate increases drastically as

a)

b)

Figure 7 a)Distributions of Longshore Transport Rate in Different Wave Directions
b)Comparison of Longshore Transport Rates between CERC Formula and Present Model in Different Wave Directions.

wave angle increases. The total transport rate is obtained by integrating the volume under the curves. These total transport rates are compared with the CERC's formula in Figure 7(b) which plots the transport rate *vs.* wave height for different wave angles. The comparisons are good for wave up to 20°. For larger wave angles, the model yields values slightly higher than the CERC's formula. The coefficient A_{bc} in the transport equation given by Equation (6) is equal to unity and 0.77 was used for the K value of CERC formula in this comparisons. As discussed earlier, most experiments and field measurements were conducted for cross-shore transport, and there is very little information on longshore transport rate. Therefore, a plain beach movable bed physical model was constructed in a wave basin to investigate the sediment transport patterns , specially longshore transport rate. The experiments were performed in the 16x23 *m* 3-D wave basin of the Coastal Engineering Laboratory of the Department of Coastal and Oceanographic Engineering at University of Florida. The designed initial beach profile consists of a flat backshore, a steep-sloped foreshore, and a mild-sloped offshore, and has simple straight shoreline and parallel offshore contours.

After 80 minutes run time, a total of 0.28 m^3 sand was collected at the sediment trap channel located in the downdrift boundary. This longshore transported material was used to calibrate the A_{bc} value in the numerical model and to check the K value in CERC's formula. By applying wave height, and angle used in the experiment to the CERC's formula, it was found that $K=0.23$ from the results. This value of the proportionality coefficient obtained in this study is smaller than 0.77 in Komar and Inman's formula and is rather close to the value in Sato and Tanaka (1966)'s formula. It is noted here that many one line models utilizing CERC's formula the K coefficient was adjusted downward to the range of 0.05 - 0.4 based on model calibrations with physical experiment data. Here, the numerical longshore sediment transport is calibrated with measured total longshore transport quantitatively. The best fitting value was found to be $A_{bc} = 0.1$. This value is also smaller than the previous value which gave good agreement with CERC's formula.

Performance Test

The model performance is demonstrated here with two types of man-made structures including shore perpendicular structures(groins) and offshore breakwaters. The purpose is not for model calibration or verification as there is no available data in hand. Rather, model utilizations are illustrated with realistic coastal structures.
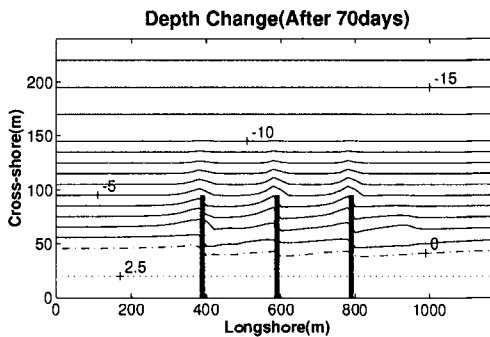
Groins

Groins are shore perpendicular structures which are built to intercept littoral transport from updrift. They are used to trap sand locally or as end structures to stabilize sand placed in conjunction with beach nourishment projects. For trapping sand, a series of groins is often used. The presence of groins is generally known to cause accretion on the updrift end and erosion on the downdrift end. The ability to be able to predict morphological changes associated with groin structure is undoubtedly useful in coastal engineering. Perlin and Dean (1985) developed an N-line model using a simple

wave refraction and diffraction scheme and longshore sediment transport equation to modify the topography. Kraus et al.(1994) investigated parameters governing beach response to groins and incorporated them into the so-called GENESIS model that can be used to predict shoreline changes in the presence of groins. In the present model, the presence of a groin is reflected in the boundary conditions. The boundary conditions for the groin in the sediment transport model are given as,

$$q_y(I, J_{groin} + 1) = 0, \quad \text{if} \quad q_y(I, J_{groin} + 1) > 0$$

$$q_y(I, J_{groin} - 1) = 0, \quad \text{if} \quad q_y(I, J_{groin} - 1) < 0$$

(11)

a)

b)
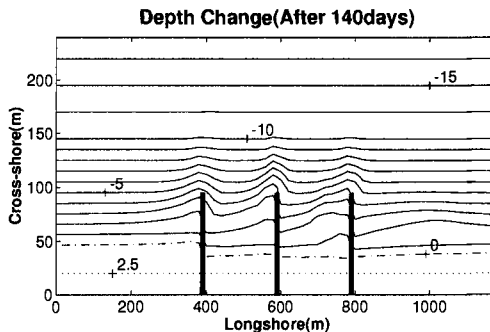
where q_y is the transport rate in y direction and J_{groin} is the Jth grid column which has the groin.

Figure 8 shows the morphological changes for the case of a three-groin after 70 days and 140 days, respectively, when wave of 0.5 m, 6 sec approaches the beach at 15 degree angle. It is shown that shoreline and bottom contours advances at the updrift of first groin and retreats at the down drift of the last groin. In each compartment, erosion occurs at the updrift end and accretion takes place at the downdrift end. At present, there is a lack of reliable data especially on the morphological effects of groins to compare with numerical results.

Figure 8 Depth Changes after a)70 days, and b)140 days on the Plain Beach with Three Groins for 0.5 m, 8 sec, and 10 degree Incident Waves.
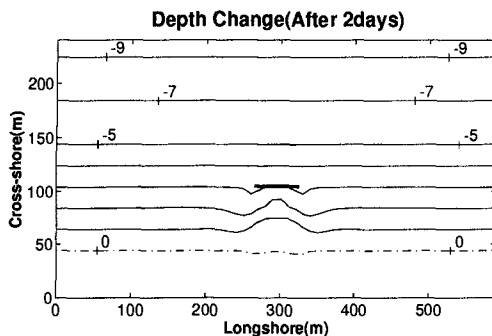
Breakwater

An offshore breakwater is generally a shore parallel structure designed to protect the beach behind the structure against severe erosion. Behind the breakwater wave

height is reduced and circulation cells are generated which draw sediment into the sheltered area. A salient feature soon appears which grows into a tombolo and sometimes becomes attached to the breakwater. Many numerical models, some based on rather artificial mechanisms are able to produce the described topographic changes. Hanson and Kraus (1990) employed a numerical model (GENESIS) to investigate the various depositional types in the lee of a single detached breakwater. Suh and Hardway (1994) developed a one-line numerical model for predicting shoreline change in the vicinity of multiple breakwaters and compared with the field data. The boundary condition for the breakwater in the present sediment transport model is as follows,
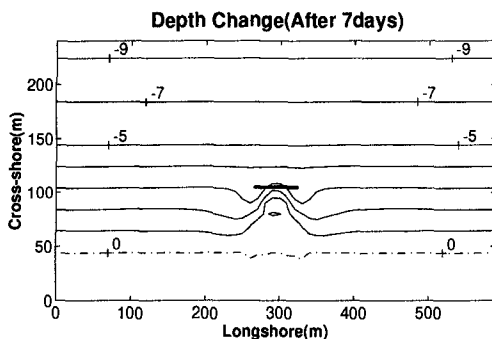
$$q_x(I_{break} + 1, J) = 0, \quad \text{if} \quad q_x(I_{break} + 1, J) > 0$$

$$q_x(I_{break} - 1, J) = 0, \quad \text{if} \quad q_x(I_{break} - 1, J) < 0 \tag{12}$$

where q_x is the transport rate in x direction and I_{break} is the Ith grid row which has the breakwater. Figure 9 shows the topographic changes after 2 days and 7 days under the normal incident wave condition with 1 m height and 8 sec period. It is clear that salient feature grows rather rapidly. Shoreline, on the other hand, changes only slightly. The absence of swash transport mechanism might be one of the reasons that shoreline change is so slight.

Inlet Experiment

The sedimentary processes in the vicinity of a tidal inlet present a complex dynamic interaction problem between fluid and sediment motion. There exist water level changes at the shoreline by tide and periodical tidal currents in and out of the inlet. This tidal current interacts with wave and wave induced longshore current. Under the combined effects of waves, longshore current, tidal current and coastal structures, the behavior of the sediment movement and morphological evolution in the inlet region is a very complicated process and the current knowledge is extremely limited. Laboratory

a)

Depth Change(After 2days)

b)

Depth Change(After 7days)

Figure 9 Depth Changes after a)2 days, and b)7 days on the Plain Beach with Breakwater for 1 m, 6 sec, and Normal Incident Waves.

modeling using movable bed-material is still a viable tool despite its limitations such as expensive cost, time consuming, and scale effects (Wang et al., 1992). Numerical model on inlet morphology is at its infancy. An attempt is made here to apply the present model to an inlet beach system. On a separate study(Wang et al., 1995), an inlet-beach physical model was constructed in the wave basin facility in the Coastal and Oceanographic Engineering Laboratory at the University of Florida. The inlet beach model consists of an idealized inlet on a plain beach with profile identical to that in the plain beach model. The inlet has two parallel jetties extending offshore with the updrift jetty twice as long as the downdrift jetty. These jetties are made of concrete blocks and impervious to sediment transport. The experiments were carried out under the condition of 7.5 degree oblique waves. The test conditions are as follows:

Wave condition: 8 cm wave height, 1 sec wave period, 7.5° wave direction
Current condition: 0.14 m/sec ebb current, 0.1 m/sec flood current
Tidal range(between flood and ebb): 3 cm
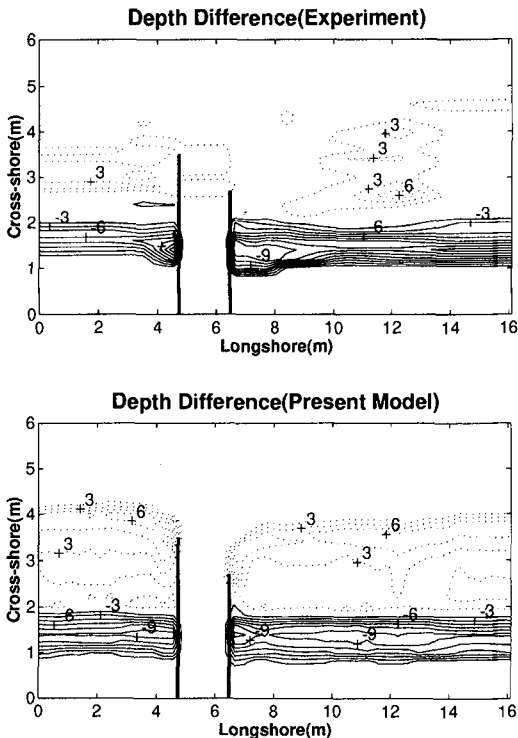
The flood and ebb tidal conditions were simulated alternatively in the model at every 40 minute intervals by holding the high and low water levels, respectively, and reversing tidal currents in the inlet. Figure 10 shows the changes of the topographies by plotting the difference between the initial contours and the contours after 160 minutes. The numerical model appears to be able to reproduce reasonably well some of the general features found in the physical model, as the locations of erosion and accretion, the position and size of breakpoint bars and the shoreline offset. Detailed topographic comparisons are still difficult and may not be too meaningful owing partly the three dimensional effects produced in the physical model.

Figure 10 Comparison of Bathymetric Changes after 160 minutes between Experiment and Numerical Model for 8 cm, 1 sec, and Oblique Incident Waves.

Results

1) The prediction of cross-shore transport from model was compared to the evolution of beach profiles and sediment transport rate distributions in the 2-D German's Big Wave Flume tests and CERC's large tank tests. The model is capable of predicting the growth and movement of main breakpoint bars and beach processes with reasonable reliability.

2) The comparison of longshore transport rates between present model and CERC formula shows close agreement for different wave angles when the coefficient $A_{bc}=1$ is adopted in the model as compatible with K=0.77 in CERC's formula. A different calibration using 3-D basin experiments yields $A_{bc}=0.1$ and K=0.23.

3) An application of the model to different coastal structures including groins and breakwaters shows the model is capable of producing the general scouring, accretion and erosion features found in nature. The model was tested with inlet beach movable bed physical model experiment. The comparison of depth changes shows reasonable agreement between numerical model and physical experiment.

References

Briand, M.-H.G. and Kamphuis, J.W., 1993a. ``Waves and currents on natural beaches: a quasi 3-D numerical model", Coastal Eng., 20:101-134.

Briand, M.-H.G. and Kamphuis, J.W., 1993b. ``Sediment transport in the surf zone: a quasi 3-D numerical model", Coastal Eng., 20:135-156.

Dally, W. R. and Dean, R. G., 1984. ``Suspended sediment transport and beach profile evolution", Journal of Waterway, Port, Coastal and Ocean Engineering, Vol.109, No. 4. pp.401-405.

Dally, W. R., Dean, R. G. and Dalrymple, R. A., 1984. ``A model for breaker decay on beaches", Proc. 19th Coastal Eng. Conf., Houston, pp.82-98.

Dette, H.H. and Uliczka, K., 1986.``Seegangserzeugte Wechselwirkung Zwischen Vorland und Vorstrand und Kustenschutzbauwerk", Technisher Bericht SFB 205/TPA6, University Hannover.

De Vriend, H.J. and Stive, M.J.F., 1987. ``Quasi-3D modeling of nearshore currents", Coastal Eng., 11;pp.565-601.

Ebersole, B.A. and Dalrymple, R.A., 1979. ``A numerical model for nearshore circulation including convective accelerations and lateral mixing", Ocean Engineering Report No. 21, Dept. of Civil Eng., Univ. of Delaware, Newark, Delaware.

Glavin, C.J., 1969. ``Breaker travel and choice of design wave height", Journal of Waterway, Port, Coastal and Ocean Engineering, ASCE, Vol.95, No. 2. pp.175-200.

Hanson, H. and Kraus, N.C. 1990. ``Shoreline response to a single transmissive detached breakwater", Proc. 22th, ICCE, ASCE pp. 2034-2046.

Horikawa, K., 1988., ``Nearshore dynamics and coastal processes ", University of Tokyo Press, pp. 522.

Kraus, N.C., Hanson, H., and Blomgren, S.H. 1994., ``Modern functional design of

groin systems", Proc. 24th, ICCE, ASCE, pp.1327-1342.

Kriebel, D. L., 1985. ``Numerical simulation of time-dependent beach and dune erosion'',Coastal Eng., Vol 9, pp. 221-245.

Larson, M., Kraus, N. C. and Byrnes, M. R., 1989. ``SBEACH: Numerical Model for Simulating Storm-Induced Beach Change'', Technical Report CERC-89-9, Coastal Engineering Research Center, US Army Corps of Engineers.

Ohnaka, S. and Watanabe, A., 1990. ``Modeling of Wave-Current Interaction and Beach Change'', Proc. 22nd Coastal Eng. Conf., Delft, The Netherlands, pp. 2443-2456.

O'Shea, K.F., Nicholson, J. and O'Connor, B.A., 1991., ``Analysis of existing laboratory data to find expression for the transition zone length'', Report MCE/1, Dept. Civil Eng., University of Liverpool, UK.

Perlin, M., and Dean, R.G., 1985. ``3-D model of bathymetric response to structures,'' Journal of Waterway, port, coastal and ocean engineering. Vol.111, No.2, pp.153-170.

Sato, S. and Tanaka, N., 1966. ``Field investigation on sand drift at Port Kashima facing the Pacific Ocean'', Proc. 10th Coastal Eng. Conf., pp. 595-614.

Saville, T., 1957. ``Scale Relationship for Equilibrium Profiles'', Int. Assoc. of Hydraulic Research, 1957

Shore Protection Manual, 1984(4th edition). Coastal Engineering Research Center, U.S. Army Corps of Engineers, Vicksburg.

Suh, K.D. and Hardaway C.S. 1994., ``Calculation of Tombolo in Shoreline Numerical Model'', Proc. 24th, ICCE, ASCE, pp. 2653-2667.

van Rijn, L.C. and Meijer, K., 1989. ``Three dimensional mathematical modeling of suspended sediment transport in currents and waves'', IAHR Symp., Copenhagen, Denmark.

Watanabe, A., Maruyama, K., Shimizu, T., Sakakiyama, T., 1986. ``Numerical prediction model of three dimensional beach deformation around a structure'', Coastal Eng. in Japan. 29, pp.179-194.

Wang, H., Lin, L., Zhong, H., and Miao, G., 1992, ``Sebastian Inlet Physical Model Studies, Part II --- Movable Bed Model'', Coastal and Oceanographic Engineering Department, University of Florida. UFL/COEL--91/014.

Wang, H., Lin, L., Zhong, H., and Wang Xu, 1995, ``Laboratory Mobile Bed Model Studies on Inlet , Part II---Ebb Tidal Shoal Evolution Process'', Coastal and Oceanographic Engineering Department, University of Florida. UFL/COEL--95/021.

Winer, H.S., 1988. ``Numerical Modeling of Wave-Induced Currents Using a Parabolic Wave Equation'', Ph.D. Dissertation, Coastal and Oceanographic Engineering Dept. Univ. of Florida.